



Aerobic oxidation of thioglycol catalysed by metallophthalocyanine in an organic-inorganic hybrid vesicle “cerasome”



Guolin Zhang^a, Li Zhang^a, Dan Zhang^a, Qiuhua Wu^a, Yoshihiro Sasaki^b, Yoshio Hisaeda^c, Kazuma Yasuhara^d, Jun-ichi Kikuchi^{d,*}, Xi-Ming Song^{a,*}

^a Liaoning Key Laboratory for Green Synthesis and Preparative Chemistry of Advanced Materials, College of Chemistry, Liaoning University, Shenyang 110036, China

^b Department of Polymer Chemistry, Graduate School of Engineering, Kyoto University, Katsura, Nishikyo-ku, Kyoto 615-8510, Japan

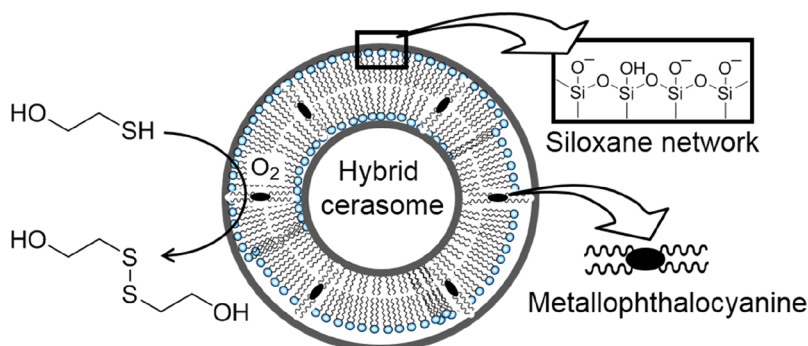
^c Department of Chemistry and Biochemistry, Graduate School of Engineering, Kyushu University, 744 Motoooka, Nishi-ku, Fukuoka 819-0395, Japan

^d Graduate School of Materials Science, Nara Institute of Science and Technology, 8916-5 Takayama, Ikoma, Nara 630-0192, Japan

GRAPHICAL ABSTRACT

A graphical and textural abstract for the Table of contents entry.

A molecular assembly of a hydrophobized metallophthalocyanine derivative embedded in a cerasome, an organic-inorganic hybrid vesicle with a lipid bilayer and silica surface, was a potent catalyst for aerobic oxidation of thioglycol.



ARTICLE INFO

Keywords:

Cerasome
Organic-inorganic hybrid vesicle
Aerobic oxidation of thioglycol
Catalytic activity

ABSTRACT

A molecular assembly of a hydrophobized metallophthalocyanine derivative embedded in a cerasome, an organic-inorganic hybrid vesicle with a lipid bilayer and silica surface, was a potent catalyst for aerobic oxidation of thioglycol. The catalytic activity was higher than those in hexadecyl 2-hydroxy-3-chloropropyl phosphate vesicles, sodium dodecylsulfate micelles, ethanol, and benzene.

1. Introduction

A lipid bilayer membrane is a basic structural component of bio-membranes, which provide a platform for systematic chemical

reactions for material and energy conversion and information processing. Until now, much effort has been paid to the development of intelligent reaction fields inspired by self-assembled biological systems using phospholipid liposomes and synthetic lipid vesicles as a

* Corresponding authors.

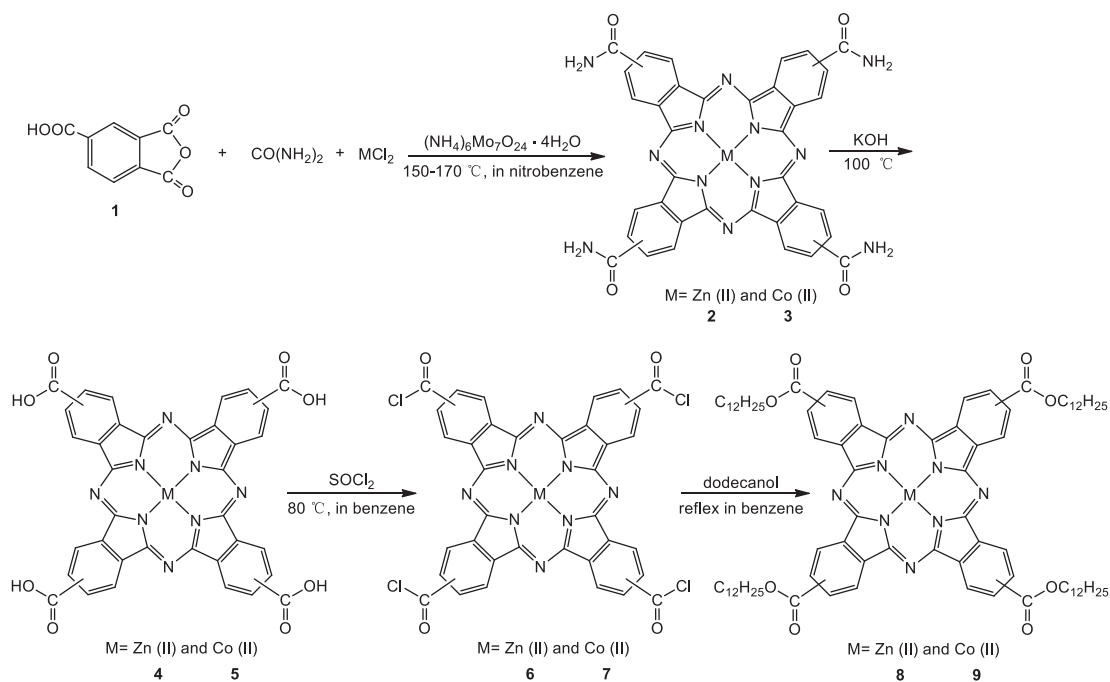
E-mail addresses: sasaki.yoshihiro.8s@kyoto-u.ac.jp (Y. Sasaki), yhisatcm@mail.cstm.kyushu-u.ac.jp (Y. Hisaeda), jkikuchi@ms.naist.jp (J.-i. Kikuchi), songlab@lnu.edu.cn (X.-M. Song).

<https://doi.org/10.1016/j.inoche.2020.107866>

Received 25 December 2019; Received in revised form 1 March 2020; Accepted 1 March 2020

Available online 03 March 2020

1387-7003/ © 2020 Elsevier B.V. All rights reserved.



Scheme 1. Synthesis of (2,9,16,23-tetrakis(dodecoxycarbonyl)phthalocyanato) zinc(II) (ZnPc) or cobalt(II) (CoPc).

membrane matrix in aqueous media [1–6]. As for the material conversion in artificial lipid membranes, a membrane matrix that has morphological stability should be employed. We have previously reported that bilayer vesicles formed with a synthetic peptide lipid and a hydrophobized coenzyme derivative of vitamin B₆ or B₁₂ exhibited significant morphological stability and effective catalytic performance as artificial enzymes [7]. To further enhance the morphological stability, we have recently developed cerasomes, lipid bilayer vesicles with a silica surface, by introducing the concept of organic–inorganic hybrid nanomaterials [8]. Although various unique characteristics of cerasomes as compared with conventional lipid bilayer vesicles have been identified, the potential of using cerasomes as catalytic reactors is uncertain. In this communication, we report the preparation of a hybrid cerasome with metallophthalocyanine reaction sites and its catalytic performance for aerobic oxidation of thioglycol.

2. Experimental

2.1. Synthesis of Zn(II) or Co(II)-4,4',4'',4'''-tetraamide phthalocyanine (Zn(II)-taPc or Co(II)-taPc)

The metallophthalocyanines were synthesized according to a literature method [9]. 5.0 g (0.025 mol) of trimellitic anhydride (1), 15.0 g (0.25 mol) of urea, 0.015 mol of the metal salt (ZnCl₂ or CoCl₂), 0.5 g (4.0 × 10⁻⁴ mol) of ammonium molybdate, and 75 mL of nitrobenzene were placed in a 200 mL round-bottomed flask and maintained at 150–170 °C for 3 h under stirring. The reaction mixture was filtered to give a blue-black solid, which was washed with 100 mL of methanol. The crude product was soaked in 100 mL of 6 mol/L HCl aqueous solution under stirring for 1 h and then filtered. The procedure was repeated three times. The product was washed with distilled water, methanol, and diethyl ether and then dried under vacuum to give the product as a blue-black solid. Zn(II)-taPc (2): yield: 82%. Co(II)-taPc (3): yield: 86%.

2.2. Synthesis of Zn(II)-4,4',4'',4'''-tetracarboxy phthalocyanine (Zn(II)-tcPc or Co(II)-tcPc)

5.0 g of Zn(II)-taPc (or Co(II)-taPc) and 200 mL of 50% KOH(aq)

were placed in a 500 mL round-bottomed flask and refluxed at 100 °C for 12 h under stirring. The reaction mixture was diluted with 500 mL distilled water and filtered through a glass sand funnel. The pH of the filtrate was regulated to 2 with a 12 mol/L HCl aqueous solution to give a dark blue cotton-shaped precipitate. The mixture allowed to stand overnight and was then filtered through a glass sand funnel. The solid was washed with 0.1 mol/L HCl, distilled water, acetone, and diethyl ether, and then dried under vacuum to give Zn(II)-tcPc (or Co(II)-tcPc). Zn(II)-tcPc (4): yield: 23%. Co(II)-tcPc (5): yield: 49%.

2.3. Synthesis of Zn(II)- or Co(II)-tcPc tetraacid chloride

A solution containing 1.13 g (0.0015 mol) of Zn(II)-tcPc (or 1.12 g (0.0015 mol) of Co(II)-tcPc), 5.5 mL (0.07 mol) of thionyl chloride, a few drops of pyridine, and 50 mL of benzene was refluxed for 10 h under stirring. The product was filtered off, washed with benzene, and dried at 70 °C under vacuum to give Zn(II)-tcPc tetraacid chloride (or Co(II)-tcPc tetraacid chloride). Zn(II)-tcPc tetraacid chloride (6): yield: 93%. Co(II)-tcPc tetraacid chloride (7): yield: 96%.

2.4. Synthesis of (2,9,16,23-tetrakis(dodecoxycarbonyl) phthalocyanato) zinc(II) (ZnPc) or cobalt(II) (CoPc)

A solution containing 1.0 g (0.0012 mol) of Zn(II)-tcPc tetraacid chloride (or 0.98 g (0.0012 mol) Co(II)-tcPc tetraacid chloride), 2.3 g (0.012 mol) of dodecanol, a few drops of pyridine, and 50 mL of anhydrous benzene was refluxed for 15 h under stirring. The mixture was filtered through a glass sand funnel. The precipitate was washed with chloroform until the filtrate was colourless. The filtrate was combined and concentrated by rotary evaporator to obtain a blue-black solid, which was dried under vacuum. The product was purified by column chromatography with silica gel (CH₃CH₂OH/CHCl₃ = 3:1 v/v). ZnPc (8): yield: 5.1%. CoPc (9): yield: 15.3%. The reaction route is shown in Scheme 1.

2.5. Preparation of hybrid cerasome

The hybrid cerasome was prepared from a cerasome-forming lipid, *N,N*-dihexadecyl-*N*^α-(6-((3-triethoxysilyl)propyl)dimethylammonio)

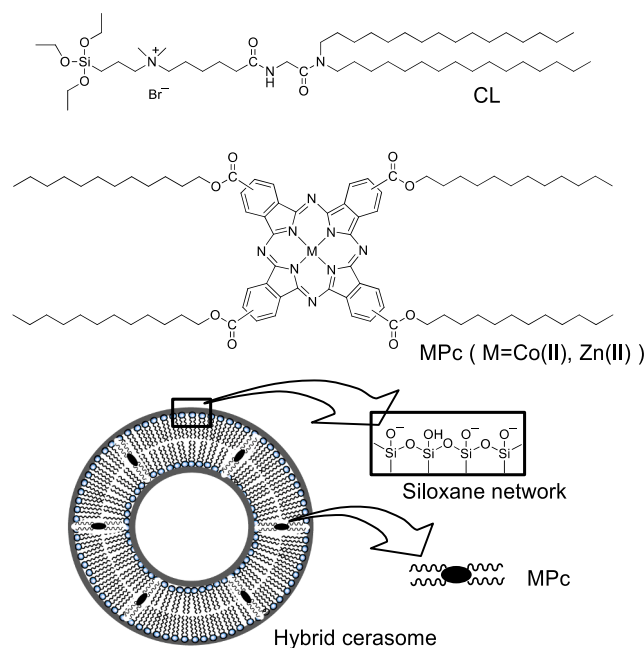


Fig. 1. Structures of cerasome-forming lipid (CL) and metallophthalocyanine (MPc) derivatives and a schematic image of a hybrid cerasome.

hexanoyl)glycinamide bromide (CL) [10] and a hydrophobized metallophthalocyanine derivative (MPc), (2,9,16,23-tetrakis(dodecoxy-carbonyl)phthalocyanato)cobalt(II) (CoPc) or (2,9,16,23-tetrakis(dodecoxy-carbonyl)phthalocyanato)zinc(II) (ZnPc) (Fig. 1). In a glass vessel, appropriate amounts of CL and MPc were dissolved in chloroform and evaporated to give a homogeneous mixture. This mixture was dispersed in 2-[4-(2-hydroxyethyl)piperazin-1-yl]ethanesulfonate (HEPES) buffer (25 mM, pH 7.0) by vortex mixing and followed by sonication with a groove-type sonicator at 100 W power for 10 min to give a translucent cerasome solution.

3. Results and discussion

3.1. Synthesis of Zn(II)-taPc or Co(II)-taPc

In the IR spectrum of Zn(II)-taPc (**2**), the peak at 1668 cm^{-1} comes from the C=O stretching vibration of $-\text{CO}-\text{NH}_2$ segment. The peaks at $1615, 1525, 1351, 1092, 767, 713\text{ cm}^{-1}$ are assigned to the characteristic absorption of phthalocyanine macrocycle. Anal. calcd for $\text{C}_{36}\text{H}_{20}\text{N}_{12}\text{O}_4\text{Zn}$: C, 57.65%; H, 2.69%; N, 22.41%. Found: C, 57.35%; H, 2.74%; N, 21.86%. In the IR spectrum of Co(II)-taPc (**3**), the peak at 1659 cm^{-1} comes from the C=O stretching vibration of $-\text{CO}-\text{NH}_2$ segment. The peaks at $1618, 1516, 1324, 1083, 771, 738\text{ cm}^{-1}$ are assigned to the characteristic absorption of phthalocyanine macrocycle. Anal. calcd for $\text{C}_{36}\text{H}_{20}\text{N}_{12}\text{O}_4\text{Co}$: C, 58.15%; H, 2.71%; N, 22.61%. Found: C, 58.42%; H, 2.89%; N, 22.38%.

3.2. Synthesis of Zn(II)-tcPc or Co(II)-tcPc

In the IR spectrum of Zn(II)-tcPc (**4**), the peak at 1705 cm^{-1} comes from the C=O stretching vibration of $-\text{COOH}$ group. The peaks at $1610, 1332, 1086, 765, 737\text{ cm}^{-1}$ are assigned to the characteristic absorption of phthalocyanine macrocycle. Anal. calcd for $\text{C}_{36}\text{H}_{16}\text{N}_8\text{O}_8\text{Zn}$: C, 57.34%; H, 2.14%; N, 14.86%. Found: C, 57.25%; H, 2.42%; N, 14.37%. In the IR spectrum of Co(II)-tcPc (**5**), the peak at 1705 cm^{-1} comes from the C=O stretching vibration of $-\text{COOH}$ group. The peaks at $1613, 1383, 1094, 785, 744\text{ cm}^{-1}$ are assigned to the characteristic absorption of phthalocyanine macrocycle. Anal. calcd for $\text{C}_{36}\text{H}_{16}\text{N}_8\text{O}_8\text{Co}$: C, 57.84%; H, 2.16%; N, 14.99%. Found: C, 57.56%; H,

2.53%; N, 14.75%.

3.3. Synthesis of Zn(II)- or Co(II)-tcPc tetraacid chloride

In the IR spectrum of Zn(II)-tcPc tetraacid chloride (**6**), the peak at 1716 cm^{-1} comes from the C=O stretching vibration of $-\text{COCl}$ segment. The peaks at $1637, 1506, 1471, 1082, 777, 678\text{ cm}^{-1}$ are assigned to the characteristic absorption of phthalocyanine macrocycle. Anal. calcd for $\text{C}_{36}\text{H}_{12}\text{N}_8\text{O}_4\text{Cl}_4\text{Zn}$: C, 52.23%; H, 1.46%; N, 13.54%. Found: C, 52.59%; H, 1.27%; N, 13.29%. In the IR spectrum of Co(II)-tcPc tetraacid chloride (**7**), the peak at 1701 cm^{-1} comes from the C=O stretching vibration of $-\text{COOH}$ segment. The peaks at $1636, 1521, 1476, 1088, 744, 678\text{ cm}^{-1}$ are assigned to the characteristic absorption of phthalocyanine macrocycle. Anal. calcd for $\text{C}_{36}\text{H}_{12}\text{N}_8\text{O}_4\text{Cl}_4\text{Co}$: C, 52.65%; H, 1.47%; N, 13.64%. Found: C, 52.43%; H, 1.51%; N, 13.35%.

3.4. Synthesis of ZnPc or CoPc

In the IR spectrum of ZnPc (**8**), the peak at 1700 cm^{-1} comes from the C=O stretching vibration of $-\text{COOC}_{12}\text{H}_{25}$ segment. The peaks at $1625, 1577, 1387, 1090, 737\text{ cm}^{-1}$ are assigned to the characteristic absorption of phthalocyanine macrocycle. The ^1H NMR spectrum of ZnPc (**8**) is shown in Fig. 2A. The peak at 0.87 ppm is assigned to protons a in the $-\text{CH}_3$ segments. The peaks at 1.26–1.91 ppm are assigned to protons b in the $-(\text{CH}_2)_{10}\text{CH}_3$ segments. The peak at 4.03 ppm is assigned to protons c in the $-\text{CH}_2\text{O}-$ segments. The peak at 7.26 ppm is assigned to protons d in the Ph-H segments. Anal. calcd for $\text{C}_{84}\text{H}_{112}\text{N}_8\text{O}_8\text{Zn}$: C, 70.69%; H, 7.91%; N, 7.85%. Found: C, 70.51%; H, 7.64%; N, 7.71%. In the IR spectrum of CoPc (**9**), the peak at 1716 cm^{-1} comes from the C=O stretching vibration of $-\text{COOC}_{12}\text{H}_{25}$ segment. The peaks at $1626, 1491, 1365, 1094, 729\text{ cm}^{-1}$ are assigned to the characteristic absorption of phthalocyanine macrocycle. The ^1H NMR spectrum of CoPc (**9**) is shown in Fig. 2B. The peak at 0.88 ppm is assigned to protons a in the $-\text{CH}_3$ segments. The peaks at 1.26–1.95 ppm are assigned to protons b in the $-(\text{CH}_2)_{10}\text{CH}_3$ segments. The peak at 3.64 ppm is assigned to protons c in the $-\text{CH}_2\text{O}-$ segments. The peak at 7.26 ppm is assigned to protons d in the Ph-H segments. Anal. calcd for $\text{C}_{84}\text{H}_{112}\text{N}_8\text{O}_8\text{Co}$: C, 71.01%; H, 7.94%; N, 7.89%. Found: C, 71.18%; H, 7.72%; N, 7.67%.

3.5. Preparation of hybrid cerasome

The hydrodynamic diameter of the hybrid cerasome evaluated by dynamic light scattering measurements was $500 \pm 25\text{ nm}$. Optical microscopy images of hybrid cerasomes formed with CL and ZnPc are shown in Fig. 3. The cerasome particles were observed in both phase contrast mode and fluorescence mode using an optical light filter U-MWU2 ($\lambda_{\text{ex}}, 330\text{--}380\text{ nm}$; $\lambda_{\text{em}}, > 450\text{ nm}$). A similar particle image was also observed in phase contrast mode for the hybrid cerasomes containing 1–5 mol% of non-fluorescent CoPc. Although the image of MPc-free cerasomes was also confirmed by phase contrast microscopy, no particles were detected in the fluorescence mode. Because the MPc derivatives were insoluble in water, the results indicated that CL and MPc formed the corresponding hybrid cerasomes.

The microenvironment around the MPc in the cerasomes was evaluated by electronic spectroscopy. The UV-vis absorption spectrum of hybrid cerasomes formed with CL and CoPc is shown in Fig. 4A. The absorption maximum at 675 nm was assigned to the monomeric CoPc species, based on our previous report that a MPc, (2,9,16,23-tetrakis(propoxy-carbonyl)phthalocyanato)cobalt(II), is present as a monomer with a maximum absorption at 680 nm in benzene and the aqueous vesicle formed with hexadecyl 2-hydroxy-3-chloropropyl phosphate (HHP) or as a dimer with broad absorption at 620 nm in ethanol and a aqueous micelle of sodium dodecyl sulfate (SDS) [11].

The ZnPc in the cerasomes showed fluorescence with an emission

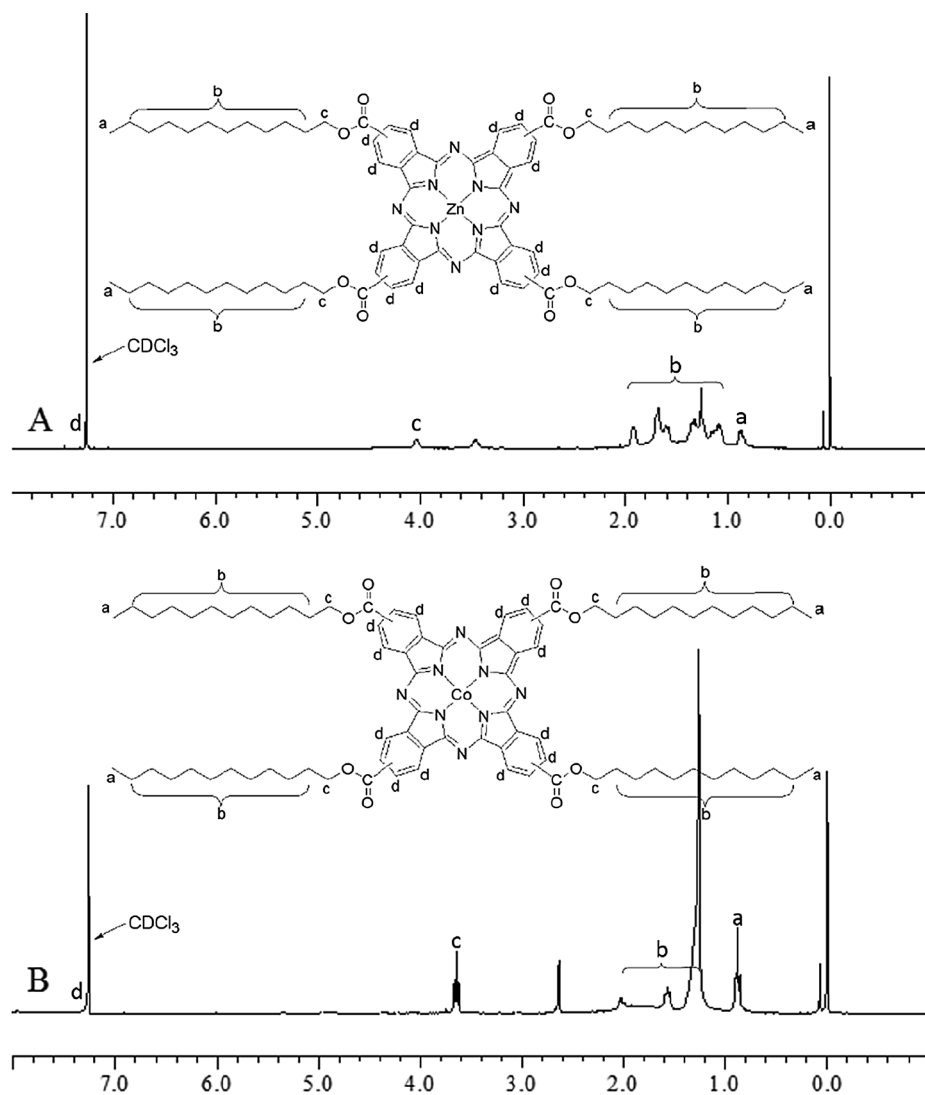


Fig. 2. ^1H NMR spectra of ZnPc (A) and CoPc (B) in CDCl_3 .

maximum at 704 nm (Fig. 4B). Since the maximum emission wavelength of ZnPc depends on the solvent polarity, we can evaluate the microenvironmental polarity around ZnPc in the cerasomes. Thus, it became apparent that the cerasomes provided a hydrophobic microenvironment similar to that in dioxane for ZnPc. This is comparable to the HHP vesicular system in which ZnPc was placed in a polar microenvironment similar to that in benzene and the emission maximum was

680 nm. The results indicated that MPc molecules were distributed homogeneously in a hydrophobic region of the cerasomes without the formation of aggregates.

3.6. Catalytic properties of hybrid cerasome

MPc compounds are synthetic aromatic metal complexes that

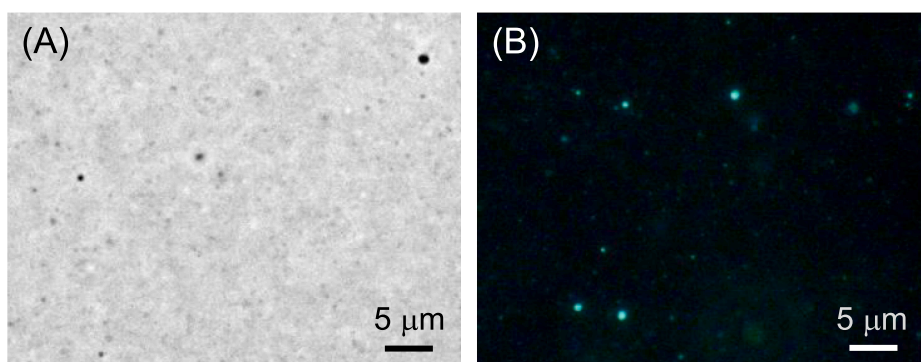


Fig. 3. Optical microscopy images of hybrid cerasomes formed with CL (1.0 mmol dm^{-3}) and ZnPc ($0.05 \text{ mmol dm}^{-3}$) in HEPES buffer (25 mmol dm^{-3} , pH 7.0) at 25°C : (A) phase contrast mode, (B) fluorescence mode.

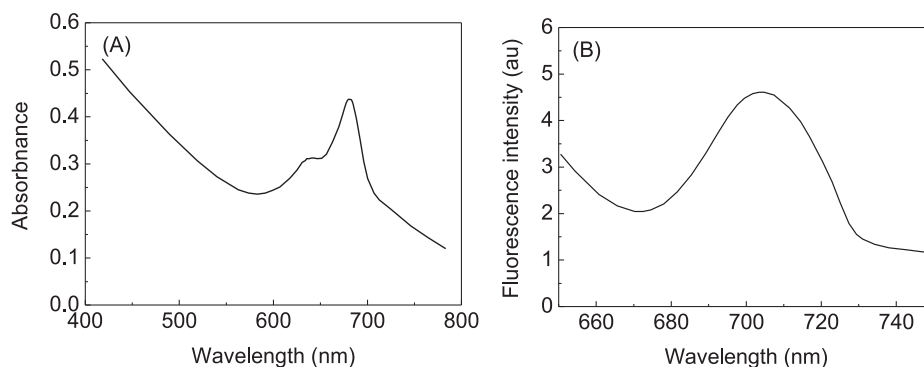


Fig. 4. UV-vis spectra of CoPc hybrid cerasome (A) and fluorescence spectra of ZnPc hybrid cerasome (B) in HEPES buffer (25 mmol dm⁻³, pH 7.0) at 25 °C: [CL], 1.0 mmol dm⁻³; [MPc], 0.01 mmol dm⁻³.

possess catalytic performance towards a wide variety of reactions [12,13]. Mercapto compound can be oxidized to produce disulfides as: $4\text{RSH} + \text{O}_2 \rightarrow 2\text{RSSR} + 2\text{H}_2\text{O}$. The oxidation can be catalysed by MPC complexes. The reaction has significance not only to clarify the catabolic mechanism of sulfhydryl compounds in biological system but also to develop novel active deodorant catalysts in industrial fields. On these grounds, we evaluated the catalytic activity of hybrid cerasomes formed with CL and CoPc for the aerobic oxidation of a sulfhydryl compound. Thioglycol was the select sulfhydryl compound and the oxidation product was diethyl disulfide. The oxidation reaction was followed by oxygen consumption with a Warburg respirometer [9,11].

Fig. 5A shows time courses of oxygen consumption for the aerobic oxidation of thioglycol in cerasome, as prepared or after incubation overnight at room temperature, in the presence and absence of CoPc. Although the non-catalytic oxidation of thioglycol by dissolved oxygen proceeded gradually in CoPc-free cerasomes, we observed extremely high catalytic activity of hybrid cerasomes containing CoPc. We have previously clarified that the development of a siloxane network on the cerasome surface depends on the incubation time after the preparation of the cerasomes; that is, the siloxane network is not well developed in freshly prepared cerasomes but developed well, although not completely, after incubation overnight at room temperature, based on the surfactant resistance behaviour of the cerasomes [10]. The degree of development of the siloxane network on the cerasome surface only had a small effect on the catalytic activity of CoPc hybrid cerasomes. The results suggest that morphologically stable cerasomes can provide an effective reaction field similar to that provided by conventional lipid bilayer vesicles, even if the membrane surface of the cerasomes is covered with an inorganic siloxane network.

To study the catalytic activity of CoPc hybrid cerasomes further, we evaluated the reactivity of CoPc for the aerobic oxidation of thioglycol in various media. As shown in Fig. 5B, the catalytic activities increased in the following order: ethanol, benzene, SDS micelle, HHP vesicle, and cerasomes; the CoPc hybrid cerasomes exhibited the highest activity among CoPc in various reaction media. As mentioned above, the CoPc molecules were embedded as monomer species in a hydrophobic region of the cerasome. It is well known that solubility of oxygen is higher in apolar solvents than in polar solvents. Thus, the higher catalytic activity of the CoPc hybrid cerasomes is probably because of the increase in the local concentration of catalytically active monomeric CoPc and oxygen in the microenvironment provided by the cerasomes.

4. Conclusion

In summary, organic-inorganic hybrid vesicles were prepared by the combination of a cerasome-forming lipid and a metallophthalocyanine derivative. The hybrid cerasomes containing CoPc showed a marked improvement in catalytic activity for the aerobic oxidation of thioglycol compared with those in other reaction media, such as conventional aqueous molecular assemblies and organic solvents. Thus, morphologically stable cerasomes have the potential to provide an effective reaction field for various catalytic conversions.

Declaration of Competing Interest

The authors declare that they have no known competing financial interests or personal relationships that could have appeared to influence the work reported in this paper.

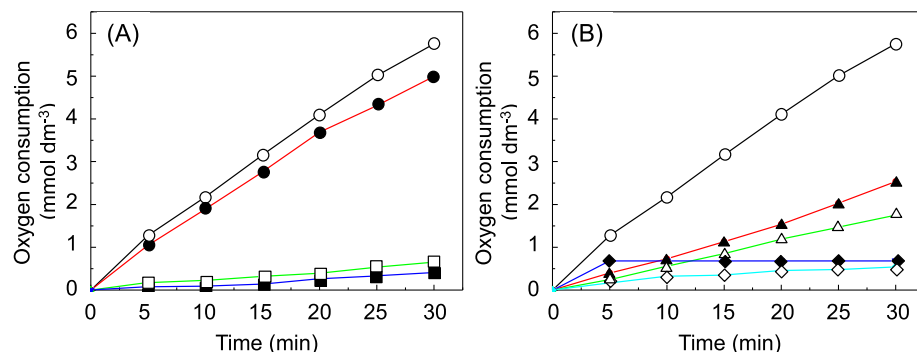


Fig. 5. Time courses of oxygen consumption for the aerobic oxidation of thioglycol in cerasomes in the presence and absence of CoPc (A) and in various reaction media containing CoPc (B) in HEPES buffer (25 mmol dm⁻³, pH 7.0) at 25 °C: [thioglycol], 570 mmol dm⁻³; [CoPc], 0.01 mmol dm⁻³; [CL], 1.0 mmol dm⁻³; [HHP], 1.0 mmol dm⁻³; [SDS], 10 mmol dm⁻³. CoPc hybrid cerasome as prepared (○) and after incubation overnight (●), freshly prepared CoPc-free cerasomes (□) and after incubation overnight (■), HHP vesicle (▲), SDS micelle (△), benzene (◆), and ethanol (◇).

Acknowledgements

This research was financially supported by the National Natural Science Foundation of China (No. 51273087) and a Grant-in-Aid for Scientific Research B (No. 25288077) from the Japan Society for the Promotion of Science (JSPS). We thank Zoran Dinev, PhD, from Edanz Group (www.edanzediting.com/ac) for editing a draft of this manuscript.

Appendix A. Supplementary material

Supplementary data to this article can be found online at <https://doi.org/10.1016/j.inoche.2020.107866>.

References

- [1] Y. Murakami, J. Kikuchi, Y. Hisaeda, O. Hayashida, *Artificial enzymes*, *Chem. Rev.* 96 (1996) 721–758.
- [2] D. Gust, T.A. Moore, A.L. Moore, *Mimicking photosynthetic solar energy transduction*, *Acc. Chem. Res.* 34 (2001) 40–48.
- [3] J. Kikuchi, K. Ariga, Y. Sasaki, in: G.W. Gokel (Ed.), *Advances in Supramolecular Chemistry*, Cerberus Press, South Miami, 2002, 131–173.
- [4] R.H. Dong, W.M. Liu, J.C. Hao, *Soft vesicles in the synthesis of hard materials*, *Acc. Chem. Res.* 45 (2012) 504–513.
- [5] G.T. Noble, R.J. Mart, K.P. Liem, S.J. Webb, in: P.A. Gale, J.W. Steed (Eds.), *Supramolecular Chemistry from Molecules to Nanomaterials*, Wiley, Chichester, 2012, 1731–1749.
- [6] P. Walde, H. Umakoshi, P. Stano, F. Mavelli, *Emergent properties arising from the assembly of amphiphiles. Artificial vesicle membranes as reaction promoters and regulators*, *Chem. Commun.* 50 (2014) 10177–10197.
- [7] Y. Murakami, J. Kikuchi, Y. Hisaeda, T. Ohno, in: J.M. Lehn, J.L. Atwood, J.E.D. Davies, D.D. MacNicol, F. Vögtle, Y. Murakami (Eds.), *Comprehensive Supramolecular Chemistry*, Elsevier Science, Oxford, 1996, 415–472.
- [8] J. Kikuchi, K. Yasuhara, in: A. George (Ed.), *Advances in Biomimetics*, InTech, Rijeka, 2011, 231–250.
- [9] H. Shirai, A. Maruyama, K. Kobayashi, N. Hojo, *Functional metal-porphyrine derivatives and their polymers. 4. Synthesis of poly(styrene) bonded Fe(III)- as well as Co(II) -4,4',4'',4'''-tetracarboxyphthalocyanine and their catalase-like activity*, *Makromol. Chem.* 181 (1980) 575–584.
- [10] K. Katagiri, M. Hashizume, K. Ariga, T. Terashima, J. Kikuchi, *Preparation and characterization of a novel organic-inorganic nanohybrid "Cerasome" formed with a liposomal membrane and silicate surface*, *Chem. Eur. J.* 13 (2007) 5272–5281.
- [11] X.M. Song, G.L. Zhang, Q.H. Wu, F.Q. Liu, P. Tian, Z.R. Liu, X.D. Zhang, F. Zhang, J. Wang, Q.T. Liu, *Novel pH and Ionic strength-sensitive vesicles composed of alkyl phosphates with 2-hydroxy-3-chloropropyl or epoxy propyl on their membrane surface*, *Chem. J. Chin. Univ.* 25 (2004) 787–789.
- [12] M. Evangelisti, in: J.L. Atwood, J.W. Steed (Eds.), *Encyclopedia of Supramolecular Chemistry*, Marcel Dekker, New York, 2004, 1069–1075.
- [13] J.H. Zagal, S. Griveau, J.F. Silva, T. Nyokong, F. Bedioui, *Metallophthalocyanine-based molecular materials as catalysts for electrochemical reactions*, *Coord. Chem. Rev.* 254 (2011) 2755–2791.